Protein Science (1994), *3*:248–256. Cambridge University Press. Printed in the USA.

Interaction of semisynthetic variants of RNase A with ribonuclease inhibitor

ULF NEUMANN AND JAN HOFSTEENGE
Friedrich Miescher-Institut, CH-4002 Basel, Switzerland

(RECEIVED August 17, 1993; ACCEPTED September 27, 1993)

Abstract

Derivatives of ribonuclease A (RNase A) with modifications in positions 1 and/or 7 were prepared by subtilisin-catalyzed semisynthesis starting from synthetic RNase 1–20 peptides and *S*-protein (RNase 21–124). The lysyl residue at position 1 was replaced by alanine, whereas Lys-7 was replaced by cysteine that was specifically modified prior to semisynthesis. The enzymes obtained were characterized by protein chemical methods and were active toward uridylyl-3′,5′-adenosine and yeast RNA. When Lys-7 was replaced by *S*-methyl-cysteine or *S*-carboxamidomethyl-cysteine, binding of recombinant ribonuclease inhibitor (RI) from porcine liver was strongly affected. In contrast, the catalytic properties were only slightly altered. The dissociation constant for the RNase A–RI complex increased from 74 fM (RNase A) to 4.5 pM (Lys-1,Cys-7-methyl RNase), corresponding to a decrease in binding energy of 10 kJ mol^{-1}. Modifications that introduced a positive charge in position 7 (*S*-aminoethyl- or *S*-ethylpyridyl-cysteine) led to much smaller losses. The replacement of Lys-1 resulted in a 4-kJ mol^{-1} loss in binding energy. *S*-protein bound to RI with $K_i \approx 63.4$ pM, 800-fold weaker than RNase A. This corresponded to a 16-kJ mol^{-1} difference in binding energy. The results show that the N-terminal portion of RNase A contributes significantly to binding of ribonuclease inhibitor and that ionic interactions of Lys-7 and to a smaller extent of Lys-1 provide most of the binding energy.

Keywords: protein–protein interaction; ribonuclease; ribonuclease inhibitor; semisynthesis

Pancreatic ribonucleases (RNases) form very tight and stoichiometric complexes with a 50-kDa cytosolic protein called ribonuclease inhibitor (RI). The primary structures of RI from human placenta, pig liver, and rat lung have been determined. RI consists of 15 leucine-rich repeats and contains 30 (porcine liver) or 32 (human placenta) free cysteinyl residues (for a recent review, see Lee & Vallee, 1993). Three of the enzymes of the RNase superfamily have been studied with respect to their interaction with RI. For the RNases from bovine pancreas and human placenta as well as for the blood vessel growth-inducing protein angiogenin, dissociation constants in the femtomolar range and nearly diffusion-controlled ($>10^8$ M^{-1} s^{-1}) association rate constants were observed (Lee et al., 1989; Vicentini et al., 1990; Shapiro & Vallee, 1991). A few attempts have been made to locate the interaction sites, both on the surface of the enzymes as well as on the inhibitor. Analysis of the kinetic behavior of deletion mutants and truncated forms of RI (Lee & Vallee, 1990; Hofsteenge et al., 1991a) and labeling experiments of its cysteinyl residues (Hofsteenge et al., 1991b) suggest that the C-terminal part of the inhibitor might be involved in the RNase–RI interaction.

To study the effects of RNase A modification on inhibitor binding, Blackburn and coworkers used proteolytic RNase A derivatives with truncations at both the N- and the C-terminus. For *S*-protein (RNase A 21–124, the cleavage product of controlled subtilisin action toward RNase A; Richards & Vithayathil, 1959) as well as for RNase A 1–119, no loss in inhibitor binding was observed (Blackburn & Jailkhani, 1979). It was concluded that the N-terminal part of the RNase A molecule, the so-called "*S*-peptide" region (RNase A 1–20), is not involved in RI binding. In labeling experiments in which the lysyl residues of RNase A were modified in the presence or absence of RI, a strong protection of Lys-7 (part of the *S*-peptide helix) was found in the RNase A–RI complex (Blackburn & Gavilanes, 1982). Moreover, Vallee and coworkers described an angiogenin mutant in which residues 8–22 were replaced by residues 7–21 of RNase A, and found that this hybrid protein binds at least 1 order of magnitude more strongly to RI than does wild-type

Reprint requests to: Jan Hofsteenge, Friedrich Miescher-Institut, P.O. Box 2543, CH-4002 Basel, Switzerland.

Abbreviations: RNase A, bovine pancreatic ribonuclease A; RI, ribonuclease inhibitor; UpA, uridylyl-3′,5′-adenosine; UpU, uridylyl-3′,5′-uridine; FPLC, fast protein liquid chromatography; TFA, trifluoroacetic acid; Tris, (trishydroxymethyl)aminomethane; MES, 2-(*N*-morpholino)-ethanesulfonic acid; HEPES, 4-(2-hydroxyethyl)-1-piperazinesulfonic acid; BSA, bovine serum albumin; DTT, dithiothreitol; C18, octadecylsilane; FMOC, fluorenylmethyloxycarbonyl; P2, phosphodiester group in nucleotide substrates next to the scissile bond in the 3′-direction.

angiogenin (Bond & Vallee, 1990). Very recently, it was shown that an angiogenin mutant in which Arg-5 (corresponding to Ala-4 in RNase A) had been replaced by alanine binds 50-fold more weakly to placenta ribonuclease inhibitor than does angiogenin (Shapiro & Vallee, 1993).

It seems possible that differences in affinity between RNase A and *S*-protein were overlooked in the early experiments, because they were done at protein concentrations that were 6 orders of magnitude higher than the K_i value of the RNase A–RI complex. For this reason, we reinvestigated the contribution of the N-terminus of RNase A to the interaction with ribonuclease inhibitor. These studies may contribute to the delineation of the ribonuclease-binding domain in the recently determined 3-dimensional structure of RI (Kobe & Deisenhofer, 1993).

Results

Binding of S-protein to ribonuclease inhibitor

As pointed out in the introduction, previous determinations of the strength of *S*-protein binding to RI from human placenta were performed under conditions that did not take into account the, then unknown, very tight interaction between RNase A and RI. We reinvestigated the binding of *S*-protein to recombinant RI from porcine liver using a protocol that was shown to be well suited for the competition of 2 tightly binding proteins (Stone et al., 1987). RNase A activity in a mixture with substrate and RI was found to increase in the presence of high picomolar concentrations of *S*-protein compared to the control without *S*-protein. The effect of varying concentrations of *S*-protein on the amount of free RNase A is shown in Table 1. From these results, an average K_i for the *S*-protein–RI complex of 64.7 ± 6.3 pM was calculated.

After having established the importance of the N-terminal region of RNase A for RI binding, the question arose as to which residues were involved. It was noted before that the association rate constant for the RNase A–RI complex formation is very dependent on ionic strength (Vicentini et al., 1990). So, ionic interactions between the basic RNase molecule and the acidic RI molecule can be assumed to play a role in the recognition of the 2 proteins. The *S*-peptide region of RNase A contains 4 basic amino acid residues that potentially could be involved in such an interaction. His-12 is part of the catalytic machinery and is essential for enzymatic activity, whereas Arg-10 is thought to be involved in the stabilization of the N-terminal helix via hydrogen bonding to Glu-2. In order to obtain active and undistorted enzyme variants, we decided not to substitute His-12 and Arg-10. In contrast, no catalytic functions have been assigned to Lys-1 and Lys-7. An inspection of the X-ray structure of RNase A (Richards & Wykoff, 1971) showed that at least the side chain of Lys-7 was pointing into solution and available for an intermolecular interaction. Therefore, Lys-1 and Lys-7 were tested for their contribution to the interaction with RI.

Table 1. *Effect of S-protein on the steady-state rate of UpA cleavage by RNase A in the presence of ribonuclease inhibitor: Calculation of the S-protein–RI dissociation constant*[a]

RI (pM)	*S*-protein (pM)	Steady-state rate (nM s^{-1})	Calculated K_i(*S*-protein) (pM)
12.5	0	1.594	–
0	0	20.06	–
12.5	557	3.418	43.5
12.5	836	4.587	39.8
12.5	1,115	4.43	56.4
15.2	0	0.737	–
15.2	557	2.235	75.3
15.2	836	2.931	51.4
15.2	1,115	3.04	65.2
20.3	0	0.417	–
20.3	557	0.815	97.8
20.3	863	1.36	78.1
20.3	1,115	1.782	74.8

[a] Assays were performed as described in the Materials and methods section with 10 pM RNase A and 1.7 mM UpA. K_i values were calculated as described by Stone et al. (1987).

Subtilisin-catalyzed semisynthesis of RNase A variants

For the preparation of RNase A variants, modified at Lys-1 and Lys-7, we applied the method of protease-catalyzed protein semisynthesis as an alternative to molecular biological approaches. Pancreatic ribonuclease was among the first proteins for which a protease-catalyzed resynthesis from a noncovalent precursor complex (the complex of *S*-protein and *S*-peptide is called ribonuclease S) could be demonstrated (Homandberg & Laskowski, 1979). The large protein precursor *S*-protein is readily obtained from RNase A, and RNase 1–20 (the *S*-peptide) can easily be synthesized by solid-phase methods. We decided to replace Lys-7 by a cysteinyl residue while having alanine or lysine in position 1, and to modify the cysteine with different reagents prior to the semisynthetic step in order to produce a number of variants from only 2 peptide precursors. The modification reagents were selected to introduce side chains of different sizes and physicochemical properties at position 7 of the RNase variants.

It was noted previously (Doscher & Hirs, 1967) that *S*-protein is a mixture of RNase 21–124 and RNase 22–124 and that the use of this starting material for semisynthesis gives a mixture of RNase 1–124 and des21-RNase 1–124 (Homandberg & Laskowski, 1979). Therefore, we studied different subtilisins for their ability to cleave RNase A selectively at the Ala-20–Ser-21 bond. Subtilisin BPN′ was found to produce RNase 21–124 and RNase 22–124 in nearly equal amounts, whereas subtilisin Carlsberg gave 85–90% of RNase 21–124 with only a 10–15% contamination of the shortened form. Subtilisin Carlsberg was also chosen for the synthetic reaction, which was performed under the conditions proposed by Homandberg et al. (1979), with small modifications. The subtilisin concentration was adjusted so that maximal product concentration was achieved after 24 h. The molar ratio of *S*-peptide/*S*-protein that was optimal for resynthesis was found to be 1:1. Synthetic yields drastically decreased when this ratio was increased (data not shown).

The newly synthesized RNase A variants could be separated from the *S*-protein as well as from noncovalent complex by cation-exchange FPLC with a phosphate buffer gradient. Further purification was achieved by reversed-phase HPLC. The elution behavior on the Mono S-column correlated well with the expected charge of the protein (Table 2). The overall yields of the

Table 2. *Semisynthetic RNases: Elution behavior on the Mono S column, ellipticity values from CD measurements, and yields of the synthesis*

RNase variant	Relative charge[a] at pH 6.0	Elution position[b] in FPLC (% *B*)	Ellipticity, $[\theta]_{222nm}$[c] (10^{-3} deg mol^{-1} mm^{-1})	Yield[d] (%)
RNase A (semisynthetic)	0	31	1.136	30
Ala-1-RNase	−1	25.5	n.d.[e]	18.4
Ala-1,Cys-7-methyl	−2	22	1.053	16.3
Ala-1,Cys-7-carboxamidomethyl	−2	20.5	1.071	35.5
Ala-1,Cys-7-aminoethyl	−1	22.3	1.078	27.3
Ala-1,Cys-7-ethylpyridyl	−1.7[f]	23.5	1.053	23.4
Lys-1,Cys-7-methyl	−1	26.5	1.053	25.2
Lys-1,Cys-7-carboxamidomethyl	−1	25.5	1.107	31.2
Lys-1,Cys-7-aminoethyl	0	26.3	1.150	17.9
Lys-1,Cys-7-ethylpyridyl	−0.7[f]	31	1.143	13.0

[a] Change in charge compared with RNase A.
[b] See Materials and methods for elution conditions.
[c] Measured in water at 22 °C with protein concentrations from 12 to 35 μM.
[d] Yields calculated from amino acid analysis after purification.
[e] n.d., not determined.
[f] Calculated with a pK_a of 5.6 for ethylpyridine; see Discussion.

synthesis ranged from 13 to 35%. All semisynthetic proteins were pure as judged from analysis by HPLC and SDS-PAGE. Furthermore, the amino acid analysis gave the expected composition. The proteins were subjected to N-terminal sequencing up to residue 27, which yielded only 1 sequence in each case. This showed that cleavages of other peptide bonds did not occur during semisynthesis. In no case was a deviation from the RNase A sequence found in positions 21–25. This suggests that from the *S*-protein mixture only RNase 21–124 underwent the synthetic reaction and that there was some discrimination against the shortened form RNase 22–124 in the synthesis.

To further study the structural integrity of the semisynthetic RNases, circular dichroism spectra were recorded in the far UV region. The semisynthetic modifications were located in the region of the *S*-peptide helix, the largest helix in the RNase A structure. Therefore, the ellipticity at 222 nm, which is a good measure of the helical content of a protein, should sensitively reflect alterations in the structure of the protein. All semisynthetic RNases showed identical CD spectra (see Table 2), indicating an equal content of helical structure and an intact 3D structure.

Interaction of RNase A variants with ribonuclease inhibitor

The enzyme variants were active toward the substrate UpA, which allowed a direct determination of the dissociation constant, K_i, by titrating a low concentration of the enzyme with ribonuclease inhibitor and measuring the steady-state rate of hydrolysis (Fig. 1). The experiments were performed as described by Vicentini et al. (1990), and the RI concentrations were chosen for an optimal distribution below and above the enzyme concentration. For enzyme variants for which weak binding ($K_i >$ 1 pM) was observed in preliminary experiments, the inhibitor concentration range was expanded to 10–20 times that of the enzymes. Data analysis was performed as described by Stone and Hofsteenge (1986); the K_i values in Table 3 are averages of 2 independent determinations. The results clearly showed that the replacement of both Lys-1 and Lys-7 by noncharged amino acids led to a drastic decrease in the ability of the enzyme to bind RI. The replacement of Lys-1 by alanine decreased the binding energy of the RNase–RI complex by around 4 kJ mol^{-1}, whereas the replacement of Lys-7 by a noncharged residue led to a decrease of about 10 kJ mol^{-1}. The loss in binding energy of the variant Ala-1,Cys-7-methyl RNase is comparable to that of *S*-protein (i.e., 16 kJ mol^{-1}). The modification of Cys-7 with an aminoethyl or ethylpyridyl residue led to signifi-

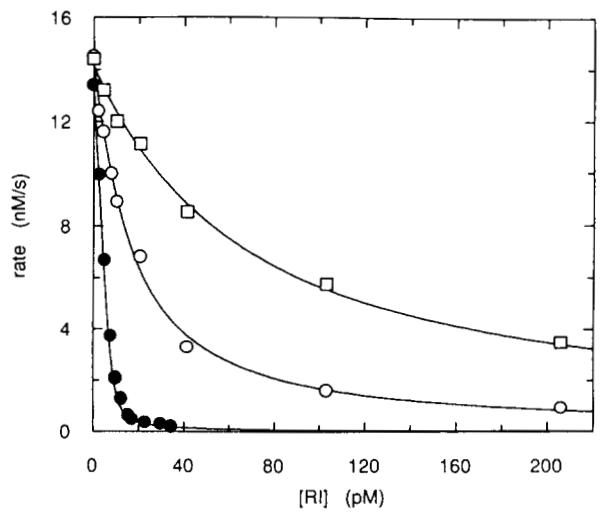

Fig. 1. Titration of RNase A (8.1 pM, full circles), Lys-1,Cys-7-methyl RNase (10 pM, open circles), and Ala-1,Cys-7-methyl RNase (10 pM, squares) with recombinant ribonuclease inhibitor. Assays were performed as described in the Materials and methods section with 1.7 mM UpA, and the observed steady-state velocities were fitted to Equation 1 to yield values for v_0, K_i', and x. The lines were drawn using these values.

Table 3. *Dissociation constants, binding energies, and binding energy differences from RNase A for the interaction of semisynthetic RNases with ribonuclease inhibitor*[a]

RNase variant	K_i (fM)	Binding energy ($-$kJ mol^{-1})	Binding energy difference from RNase A (kJ mol^{-1})
RNase A (native)	74.5	73.3	0.0
RNase A (semisynthetic)	92.5	72.8	0.5
Ala-1-RNase	447	68.9	4.4
Ala-1,Cys-7-methyl	57,700	57.2	16.2
Ala-1,Cys-7-carboxamidomethyl	30,900	58.7	14.6
Ala-1,Cys-7-aminoethyl	1,130	66.7	6.6
Ala-1,Cys-7-ethylpyridyl	1,450	66.1	7.2
Lys-1,Cys-7-methyl	4,620	63.3	10.0
Lys-1,Cys-7-carboxamidomethyl	4,650	63.3	10.0
Lys-1,Cys-7-aminoethyl	327	69.7	3.6
Lys-1,Cys-7-ethylpyridyl	559	68.4	4.9
S-protein (RNase (21–124))	63,400	57.0	16.3

[a] Values were determined in 50 mM MES, pH 6.0, with 125 mM NaCl at 25 °C as described in the Materials and methods section. Binding energies were calculated from $\Delta G = -RT \ln K_i$.

cantly stronger binding than with methyl or carboxamidomethyl substituents.

Catalytic properties of RNase A variants

To obtain further evidence that all the enzyme variants had an undistorted structure, their catalytic properties were investigated. The initial rate of cleavage of yeast RNA and the second-order rate constants for the cleavage of the dinucleoside monophosphates UpA and UpU were determined for the enzyme variants. No differences were found between native RNase A and semisynthetic RNase A, which was resynthesized from *S*-protein and native *S*-peptide. In addition to the protein chemical properties, the catalytic activity also suggests that the semisynthetic method gave completely intact protein.

The results obtained with the variants differed depending on which substrate was used. With yeast RNA, a reduction of the activity to less than 50% was observed for those variants, which had a Cys-methyl or Cys-carboxamidomethyl residue in position 7 (Table 4). Substituting alanine for lysine at position 1 resulted in a much smaller decrease in activity in all cases. The variants with Cys-7-ethylpyridyl had also markedly reduced catalytic activities, whereas the Cys-7-aminoethyl-substituted RNases had activities close to that of native RNase A.

The second-order rate constants, k_{cat}/K_m, for the substrate UpA and for UpU were determined under conditions $[S] \ll K_m$. With UpA, only slight alterations in the rate constant from 40% loss to 30% increase were observed. Again, the variants with the lowest activity were those with an uncharged side chain attached to Cys-7. Interestingly, both variants with the ethylpyridyl substitution had values higher than native RNase A. This was found twice in independent preparations. For the relatively poor RNase A substrate UpU (k_{cat}/K_m is 2 orders of magnitude lower than for UpA), a decrease in the second-order rate constant was

Table 4. *Catalytic activities of semisynthetic RNase variants toward dinucleoside monophosphates and yeast RNA*

RNase variant	k_{cat}/K_m UpA[a] (10^{-6} M^{-1} s^{-1})	k_{cat}/K_m UpU[a] (10^{-4} M^{-1} s^{-1})	Yeast RNA[b] (% of RNase A)
RNase A (native)	3.5	1.04	100
RNase A (semisynthetic)	3.3	0.94	100.2
Ala-1-RNase	3.4	0.82	87.0
Ala-1,Cys-7-methyl	2.3	0.38	31.4
Ala-1,Cys-7-carboxamidomethyl	2.1	n.d.[c]	30.2
Ala-1,Cys-7-aminoethyl	2.4	n.d.	74.8
Ala-1,Cys-7-ethylpyridyl	4.6	n.d.	34.4
Lys-1,Cys-7-methyl	2.5	0.36	43.4
Lys-1,Cys-7-carboxamidomethyl	2.5	n.d.	41.4
Lys-1,Cys-7-aminoethyl	2.9	0.52	69.4
Lys-1,Cys-7-ethylpyridyl	4.7	n.d.	42.9

[a] In 50 mM MES, pH 6.0, containing 125 mM NaCl at 25 °C.
[b] In 0.1 M Tris-HCl, pH 7.5, at 37 °C.
[c] n.d., not determined.

found for those variants in which the positive charge was removed from positions 1, 7, or both, as well as for the Lys-1,Cys-7-aminoethyl variants.

More detailed studies were carried out with the substrate UpA. For each variant, the parameters K_m and k_{cat} were determined from initial velocity measurements (Table 5). These data showed that the decrease in the second-order rate constant, k_{cat}/K_m, for the variants with uncharged side chains in position 7 was mainly due to an increase in K_m. The values for the catalytic rate constant k_{cat} were only slightly affected. In contrast, decreased values for k_{cat} were observed for the aminoethyl-substituted variants, which had K_m values indistinguishable from the native RNase A.

Discussion

Protein engineering by introducing point mutations at structurally or functionally important sites of a protein has become a well-established method for investigating catalytic mechanisms as well as protein-protein interactions (Fersht & Winter, 1992). This is almost always accomplished by site-directed mutagenesis and expression of the recombinant protein in bacteria, yeast, or mammalian cell culture. This approach allows for the replacement of amino acid residues at any desired position of a protein, but is normally restricted to the coded amino acids. Recently, a method was described that allowed the introduction of noncoded amino acids by introducing a stop codon. It used a modified tRNA that is acylated with the unnatural amino acid and has a recognition site complementary to the stop codon (Ellman et al., 1992). Another approach is the replacement of peptide fragments in a protein with the help of proteases (Chaiken, 1981). This semisynthetic approach requires the presence of a highly susceptible protease cleavage site in the native protein. Such sites are frequently found in loop structures at the surface of proteins and allow for the generation of structurally intact protein pieces. In favorable cases, this enzymatic cleavage leads to a large (protein) fragment and to a smaller (peptide) fragment. Analogues of the peptide can be synthesized by solid-phase techniques and used together with the protein fragment to resynthesize the complete protein with the help of the protease. One prerequisite for the "inverse" catalytic activity of the protease (i.e., peptide bond making instead of peptide bond breaking) is to shift the ionization status of the carboxyl component from carboxylate to carboxylic acid. Organic solvents were shown to change the pK_a's of carboxyl groups in the desired direction (Homandberg et al., 1978). A high percentage of organic co-solvent not only favors the formation of the peptide bond between the 2 precursors but also suppresses the hydrolysis of other peptide bonds. Only protein-stabilizing polyalcohols have been shown to be suited for enzyme-catalyzed semisynthesis of proteins so far. The resynthesis of a protein's peptide bond is greatly facilitated when the 2 fragments form a noncovalent complex prior to synthesis, which helps to orient the reaction partners in a favorable position. This condition is nearly ideally fulfilled for *S*-peptide and *S*-protein, which form a tight, catalytically active noncovalent complex in solution (RNase S). The crystal structures of RNase A and RNase S are superimposible except for the so called "*S*-peptide loop" (residues 15–24), the region that is cleaved in RNase S (Wlodawer et al., 1982). The "loose ends" do not seem to have a defined structure in RNase S. Although the carboxyl group of Ala-20 (C-terminus of the *S*-peptide) and the amino group of Ser-21 (N-terminus of the *S*-protein) are not in close proximity, subtilisin Carlsberg was able to form the peptide bond in 90% glycerol in moderate yields. Synthesis did not occur with an *S*-peptide lacking Ala-20 (data not shown).

Both the semisynthesis and the purification protocols for the RNase variants were simple and allowed for the preparation of a series of RNases modified at positions 1 and/or 7. The products were pure and homogeneous by all protein chemical criteria. CD spectroscopy as well as the catalytic properties suggested that there were no drastic changes in overall structure and that the catalytic machinery was intact.

The major goal of the present work was to identify residues in the *S*-peptide region of RNase A that are involved in the interaction with RI. The replacement of the basic side chains of lysines 1 and 7 with noncharged ones resulted in a drastic increase in K_i (Table 3), confirming the idea that interactions between opposite charges play an important role in the formation of the complex. In RNase A, the conformation of the backbone of Lys-7 is fixed in the N-terminal helix, whereas its side chain is flexible and not directly involved in intramolecular interactions (Santoro et al., 1993). The X-ray structures show this aminoalkyl side chain to be oriented away from the surface of the RNase molecule. The loss in binding energy due to substitution of Lys-7 by the uncharged *S*-methyl cysteine or *S*-carboxamidomethyl cysteine was 10 kJ mol^{-1}. The reintroduction of a positive charge in the *S*-aminoethyl and the *S*-ethylpyridyl cysteine variants markedly increased the binding energy compared to the uncharged variants. This supported the idea that the interaction in which Lys-7 is involved might be ionic in character. A difference in affinity between RNase A and Lys-1,Cys-7-aminoethyl RNase remains, although both side chains should be nearly isosteric (formally, only a $-CH_2-$ is replaced by an -S-). We do not know whether small differences in the side chain structure lead to a change in the orientation of the terminal ammonium group and result in a weaker interaction. The binding of Cys-7-*S*-ethylpyridyl RNase variants is weaker than that of the *S*-aminoethyl cysteinyl analogs. This is certainly due to the weaker base ethylpyridine, which is only partially protonated under the conditions of the measurement. The pK_a of the eth-

Table 5. *Kinetic parameters of cleavage of uridylyl-3',5'-adenosine by RNase A and by semisynthetic RNases*[a]

RNase variant	K_m (mM)	k_{cat} (s^{-1})
RNase A (native)	0.79	2,765
RNase A (semisynthetic)	0.73	2,409
Ala-1-RNase	0.90	3,060
Ala-1,Cys-7-methyl	1.17	2,691
Ala-1,Cys-7-carboxamidomethyl	1.10	2,310
Ala-1,Cys-7-aminoethyl	0.83	1,997
Ala-1,Cys-7-ethylpyridyl	0.61	2,806
Lys-1,Cys-7-methyl	1.07	2,675
Lys-1,Cys-7-carboxamidomethyl	1.00	2,500
Lys-1,Cys-7-aminoethyl	0.75	2,156
Lys-1,Cys-7-ethylpyridyl	0.58	2,726

[a] Values were determined in 50 mM MES, pH 6.0, containing 125 mM NaCl at 25 °C as described in the Materials and methods section.

ylpyridyl group was determined to be 5.6 in the Lys-1,Cys-7-ethylpyridyl *S*-peptide by spectrophotometric titration at 254 nm, corresponding to 30% protonation at pH 6.0.

The contribution of electrostatic effects in the binding of a substrate or an inhibitor to an enzyme has been investigated in a number of examples. In subtilisin BPN′, charged residues at 2 different sites in the substrate binding cleft were replaced by site-directed mutagenesis (Wells et al., 1987). The interaction of the mutants with charged substrates was analyzed. The free energies for the enzyme–substrate ion pair interaction were found to be 7.5 and 9.6 kJ mol^{-1}. It can be assumed from the X-ray structures of complexes of subtilisin with substrate-analogous inhibitors that these ion pairs are formed in the buried interface between enzyme and ligand and are shielded from the water environment. Smaller contributions of charged residues to the binding energy were observed in a study of ionic interactions in the formation of the thrombin–hirudin complex (Betz et al., 1991). Individual acidic residues in the C-terminus of hirudin contribute from 2.3 to 5.9 kJ mol^{-1} to the binding to the positively charged thrombin exosite. The X-ray structure of the thrombin–hirudin complex showed these interactions to occur in a nonburied environment accessible to bulk water (Rydel et al., 1991). From these results, it may be concluded that there is some correlation between the binding energy provided by an ion pair interaction and its environment. Contributions to the binding energy around 10 kJ mol^{-1} may indicate a buried ion pair. When this is applied to the RNase–RI interaction, one can conclude that the interaction of Lys-7 occurs in a buried environment. The replacement of Lys-1 by Ala resulted in a loss of binding energy in the range of 4 kJ mol^{-1}. This may be explained by an ionic interaction taking place at the surface of the RI molecule. We cannot, however, exclude contributions from other effects. In contrast to Lys-7, Lys-1 is not part of the *S*-peptide helix and is more flexible in solution. Its binding to RI is probably accompanied by a much higher loss in entropy, which may reduce the free energy of binding.

The interactions of Lys-1 and Lys-7 with RI seem to be additive. The double variants Ala-1,Cys-7-methyl RNase and Ala-1,Cys-7-carboxamidomethyl RNase have lost 16 kJ mol^{-1} of binding energy; this is very close to the sum of the binding energy differences (14.4 kJ mol^{-1}) observed with the single variants, and indicates little or no interaction between the binding sites. The interaction of Lys-7 with its binding site in the RI molecule does not change the structure of the binding site for Lys-1 greatly and vice versa. This finding of structural rigidity is supported by results of CD studies in which the CD spectrum of the RNase A–RI complex was found to be indistinguishable from the sum of the individual spectra of RNase A and RI (Hofsteenge & v. Oostrum, unpubl.).

The RNase variants without positive charges at positions 1 and 7 have dissociation constants (and binding energies) very close to that observed for the *S*-protein, which lacks the whole N-terminal region. It may be concluded that the lysyl residues in positions 1 and 7 are the only structural elements of the RNase A N-terminus able to interact with ribonuclease inhibitor, although we have not yet investigated the contributions of other residues. The observation that the contribution of the *S*-peptide region to the binding energy can be attributed to interactions of Lys-1 and Lys-7 also suggests that the structure of RI binding sites in the rest of the RNase A molecule is conserved in the *S*-protein.

RI is a highly negatively charged molecule (Hofsteenge et al., 1988), and the involvement of glutamic acid and aspartic acid residues in the binding of the basic RNase seems likely. In fact, using site-directed mutagenesis we have shown that acidic residues in the C-terminus of RI contribute significantly to the binding energy (Hofsteenge & Fominaya, unpubl.). The results presented here will be of interest with respect to the recently determined 3D structure of RI (Kobe & Deisenhofer, 1993) by contributing to the delineation of the RNase binding site.

The catalytic properties of the RNase variants were investigated mainly for 2 reasons. These data, together with those from protein chemistry, were necessary to characterize the enzyme variants in terms of structure and function. Moreover, knowledge of the values of K_m of the modified enzymes was required to calculate their dissociation constants.

When the catalytic activity of the enzyme variants, modified at positions 1 and/or 7, was tested with total RNA from yeast as the substrate, a large effect of the modification was observed. Those variants in which Lys-7 was replaced with an uncharged residue (Cys-methyl, Cys-carboxamidomethyl, and, at pH 7.5, Cys-ethylpyridyl), exhibited only 30–40% of the activity of the native enzyme. This result was expected on the basis of current assumptions about the structure of substrate binding sites in RNase A (McPherson et al., 1986; de Llorens et al., 1989). It was proposed that, in addition to the primary binding sites that interact with the nucleotide substrate in the catalytic site, a number of subsites for the binding of extended regions of the substrate exist. The lysyl residue in position 7 was implicated to be involved in the binding of the phosphodiester group in the so-called P2 position (Irie et al., 1984; Parés et al., 1991). The data obtained for RNA, an extended substrate, can be explained by destruction of this substrate binding site due to replacement of Lys-7. If this would be the only function of Lys-7, the reactivity of a minimal substrate without a phosphate in the P2 position should not be affected by the modification of Lys-7. Dinucleoside monophosphates fulfill these conditions and, therefore, UpA was tested with all the enzyme variants. Although only minor effects of the modification in position 7 were observed, the data in Tables 4 and 5 show that the replacement of Lys-7 by either noncharged or charged residues affects the cleavage of dinucleotide substrates. So far, Lys-7 has not been proposed to be involved in the catalytic events during nucleotide cleavage by RNase A (Haydock et al., 1990). Even more drastic effects were observed with UpU, where the catalytic efficiencies were reduced by about 50%. The substrate UpU was chosen because it had previously been found that the replacement of Lys-7 by Leu in a noncovalent complex of *S*-protein and synthetic *S*-peptide did not affect the cleavage of this substrate (Irie et al., 1986). We were not able to reproduce these results with our semisynthetic enzymes. The removal of the charge in position 7 may influence substrate cleavage by influencing the association rate during the formation of the enzyme–substrate complex due to the altered electrostatic properties in the surroundings of the active site. In addition, the position and/or the ionization status of the active-site histidines or of Lys-41 may be affected.

The substrates UpA and UpU do not only differ greatly in the magnitude of their catalytic efficiency. It was recently shown that the corresponding inhibitors UpcA and UpcU (where the 5′ oxygen of the phosphate group is replaced by a methylene group), bind differently to RNase A (Wlodawer et al., 1993).

The 5′-uridine was found not to be bound to the adenosine-binding site in the enzyme. The different binding modes of the 2 substrates seem to correlate with their cleavage rates as well as with their different responses to modifications in the surroundings of the active site.

Materials and methods

Materials

Chromatographic media were obtained from Pharmacia. The substrate UpA was obtained from Dr. E. Darzynkiewicz, University of Warsaw, and was used after further purification by reversed-phase HPLC on a Partisil ODS-5 column (Whatman). Recombinant ribonuclease inhibitor from porcine liver expressed in *Saccharomyces cerevisiae* was used in all experiments. Its concentration was determined by titration against a known amount of RNase A under conditions in which the concentrations of both RI and RNase were orders of magnitude higher than the dissociation constant. Remaining RNase activity was determined using UpA as the substrate. *N*-(β-iodoethyl)trifluoroacetamide was obtained from Pierce; UpU, methyl-*p*-nitrobenzenesulfonate, vinylpyridine, subtilisin Carlsberg, and BPN′ as well as *S*-methyl cysteine, *S*-ethylpyridyl cysteine, *S*-aminoethyl cysteine, and *S*-carboxamidomethyl cysteine were from Sigma (St. Louis). HPLC solvents were from Fluka (Buchs). All other chemicals were of the highest purity available.

General methods

Analytical HPLC runs of peptides and proteins were performed on a Hewlett-Packard HP 1090 liquid chromatograph with an autoinjector and diode-array detector using a Vydac C18 reversed-phase column (2.1 mm diameter). Buffer A was 0.1% TFA, and buffer B was 0.085% TFA containing 70% acetonitrile. Peptides were eluted with a gradient of 0 to 50% buffer B in 60 min at a flow rate of 0.2 mL/min. Peaks were monitored at 214 nm. For the isolation of larger amounts, Vydac columns with 4.6- or 10-mm diameters were used at flow rates of 0.5 and 2.5 mL/min, respectively.

Amino acid analysis and N-terminal sequence determination

Peptides and proteins were hydrolyzed in the gas phase by 6 N HCl; the amino acids were derivatized with (dimethylamino)azobenzenesulfonyl chloride (Knecht & Chang 1986). Amino acid sequencing was performed as described previously (Hofsteenge et al., 1988) on an Applied Biosystems Model 473A sequencer.

Mass spectrometry was done on a Canyon Creek LDI 1700 matrix-assisted laser desorption mass spectrometer at the Ciba Geigy Central Research Laboratories.

Peptide synthesis

Ala-1-*S*-peptide, Ala-1,Cys-7-*S*-peptide, and Lys-1,Cys-7-*S*-peptide were synthesized using the solid-phase/FMOC strategy at the peptide synthesis facility at the Friedrich Miescher-Institut, Basel.

CD measurements were done on a Jasco J-720 spectropolarimeter at the Biocenter, University of Basel.

Modification of synthetic S-peptides

S-methylation (Heinrikson, 1971)

S-peptide with Cys at position 7 (170 nmol) was dissolved in 0.2 mL of 250 mM Tris-HCl buffer, pH 8.6, containing 3.3 mM EDTA and 25% acetonitrile. The solution was flushed with argon for 1 h, then 10 μL of a 100 mM DTT was added and the solution was allowed to stand for 2 h. Methyl-*p*-nitrobenzenesulfonate (868 μg in 20 μL acetonitrile) was added, and the solution was incubated at 37 °C for 30 min. The modified *S*-peptides were isolated by reversed-phase HPLC as described; 80–90 nmol of product were obtained. The *S*-methyl cysteine was identified in the amino acid analysis by a peak eluting between Arg and Met, which is the same position as that of the commercially available reference compound after hydrolysis and dabsylation. Ala-1,Cys-7-methyl-*S*-peptide: MW 2,098.2; found for $(M + H)^+$, 2,103.2. Lys-1,Cys-7-methyl-*S*-peptide: MW 2,155.3; found for $(M + H)^+$, 2,154.6.

Alkylation with iodoacetamide (Charbonneau, 1989)

Alkylation was done in 100 mM Tris-HCl, pH 8.1, containing 2 mM EDTA. Cys-7-*S*-peptide (500 nmol) was dissolved, flushed with argon for 1 h, and incubated with 0.05 mmol of DTT for 2 h. One hundred microliters of 1 M iodoacetamide in 0.1 N NaOH was added and allowed to react for 30 min. The products were isolated by HPLC, yielding 110 nmol of alkylated *S*-peptides. A peak eluting slightly later than Glu in the amino acid analysis was identified to be the carboxymethyl cysteine. Ala-1,Cys-7-carboxamidomethyl-*S*-peptide: MW 2,141.3; found for $(M + H)^+$, 2,142.0. Lys-1,Cys-7-carboxamidomethyl-*S*-peptide: MW 2,198.4; found for $(M + H)^+$, 2,202.0.

S-pyridylethylation (Charbonneau, 1989)

Cys-7-*S*-peptide (250 nmol) was dissolved in 100 μL of 250 mM Tris-HCl, pH 8.6, containing 1 mM EDTA; 2 μL 10% mercaptoethanol was added and incubated for 2 h at 37 °C. Vinylpyridine (2 μL) was added, and after 2 h at 37 °C the modified peptide was isolated on a preparative C18 HPLC column. Yields were higher than 90%. Most of the *S*-ethylpyridyl cysteine decomposed during acid hydrolysis for amino acid analysis (as did the reference compound), and only a small amount could be detected at a retention time of 25.1 min (which is identical to the retention time of unhydrolyzed *S*-ethylpyridyl cysteine). Ala-1,Cys-7-ethylpyridyl-*S*-peptide: MW 2,190.3; found for $(M + H)^+$, 2,190.9. Lys-1,Cys-7-ethylpyridyl-*S*-peptide: MW 2,247.4; found for $(M + H)^+$, 2,248.0.

Aminoethylation (Schwartz et al., 1980)

One hundred nanomoles of Cys-7-*S*-peptide was dissolved in 200 mM *N*-ethylmorpholine-acetate buffer, pH 8.1, and purged with argon. A 10-fold molar excess of DTT was added, and after 1 h of incubation 50 μmol of *N*-(β-iodoethyl)trifluoroacetamide (dissolved in methanol) was added in 2 portions. Analysis by HPLC after 2 h of reaction did not show any starting material left, the main portion of the isolated product being trifluoroacetyl aminoethyl-*S*-peptide. The material was treated with 0.05 M piperidine at room temperature for 2 h to give the free *S*-aminoethyl-Cys-7-*S*-peptide. The aminoethyl modification was verified by amino acid analysis; dabsyl-aminoethyl cysteine eluted at the same position as dabsyl lysine. Ala-1,Cys-7-

aminoethyl-*S*-peptide: MW 2,127.3; found for $(M + H)^+$, 2,129.9. Lys-1,Cys-7-aminoethyl-*S*-peptide: MW 2,184.4; found for $(M + H)^+$, 2,186.8.

Preparation of S-protein

One hundred milligrams of RNase A (Boehringer Mannheim) was purified on *S*-Sepharose, dialyzed against water, and lyophilized. The protein was dissolved in 6 mL of 0.1 M HEPES, pH 8.0, and put on ice; then 100 μL of 5-mg/mL subtilisin Carlsberg (Sigma) was added. After 24 h of reaction, the *S*-protein was separated on a Sephadex G-100 column by elution with 0.05 M phosphoric acid. The protein fractions were pooled, neutralized with KOH solution, and further purified by ion-exchange chromatography on *S*-Sepharose. *S*-protein was dialyzed and the protein concentration determined by amino acid analysis.

Subtilisin-catalyzed synthesis of RNase variants (50-nmol scale)

Modified *S*-peptide (50 nmol) was lyophilized in a Speedvac, then 20 μL of the *S*-protein solution (2.5 mM in 10 mM MES buffer, pH 6.0), 14 μL of buffer, and 360 μL of glycerol were added. After thoroughly mixing the solution, 16 μL subtilisin Carlsberg (freshly dissolved in buffer to give 5 mg/mL) was added. After mixing intensively, the solution was incubated for 24 h at 25 °C. The reaction was terminated by adding 400 μL of 5 mM phenylmethanesulfonyl fluoride. After incubating for an additional hour, the solution was further diluted with 800 μL of water and injected into the FPLC. A Mono S column was used with buffer A (15 mM phosphate, pH 6.0) and buffer B (300 mM phosphate, pH 6.0). Elution was achieved with a gradient of 0 to 40% buffer B in 45 min. The product fractions were concentrated in a Speedvac and injected onto a reversed-phase HPLC as described above. The protein peak at 26–31 min was collected manually, lyophilized, and taken up in 0.5 mL water. The concentration of the product was determined by amino acid analysis. Electrophoresis on SDS-polyacrylamide gels was done with the Miniprotean II cell (Bio-Rad), and proteins were stained with Coomassie brilliant blue.

Kinetic methods

All enzymatic reactions were carried out under standard buffer conditions: 50 mM MES-NaOH, pH 6.0, containing 125 mM NaCl, 1 mM EDTA, 0.1% poly(ethylene glycol) (M_r 6,000), 0.2 mM DTT, and 0.2 mg/mL bovine serum albumin at 25 °C. Reactions were usually started by addition of the enzyme after appropriate thermal equilibration. For the determination of the constants K_m and k_{cat} of UpA, as well as for the inhibition of RNases by RI, the enzymatic reactions were stopped by mixing an aliquot with an equal volume of 4 M guanidinium isothiocyanate. The concentrations of the product, adenosine, were measured by reversed-phase HPLC on a Hypersil C18 column (Shandon) with isocratic elution with 4 mM phosphate, pH 6.0, containing 5% acetonitrile at 0.8 mL/min and 40 °C. A Hewlett-Packard 1090 liquid chromatograph with autoinjector was used for all experiments. K_m and k_{cat} for the substrate UpA were determined from the initial rates at 6 substrate concentrations in the range from 0.262 to 3.75 mM. The data were fitted to the Michaelis–Menten equation using the program Enzfitter (Elsevier Biosoft, Cambridge, UK).

The second-order rate constants, k_{cat}/K_m, for uridylyl-3′,5′-uridine were determined at $[S_0] = 60$ μM and enzyme concentrations between 30 and 55 nM. Under these conditions, the consumption of the substrate (measured by HPLC after stopping the reaction as described above, but eluting with 1.5% acetonitrile) was found to be a first-order process. The value for k_{cat}/K_m was calculated from the first-order rate constant and the enzyme concentration. The catalytic activity against yeast RNA was measured in 0.1 M Tris-HCl, pH 7.5, at 37 °C with 2.5 mg/mL RNA, as previously described (Fominaya & Hofsteenge, 1992).

Steady-state inhibition constants for the RNase–RI interaction were determined using 1.7 mM uridylyl-3′,5′- adenosine as substrate and recombinant RI from porcine liver. Reactions were performed in Eppendorf tubes at an enzyme concentration of 10 pM. Ten RI concentrations were distributed below and above the RNase concentration as required. Aliquots were taken at 80 and 140 min, mixed with an equal volume of 4 M guanidinium isothiocyanate to stop the RNase, and injected into the HPLC. The areas were converted into adenosine concentrations by using a calibration curve. The obtained steady-state rates for each inhibitor concentration were fitted to the tight-binding equation (Equation 1) as described by Stone and Hofsteenge (1986):

$$v_s = (v_0/2E_t)\{[(K_i' + xI - E_t)^2 + 4K_i'E_t]^{1/2} - (K_i' + xI - E_t)\}, \quad (1)$$

where v_0 is the rate of substrate turnover in the absence of inhibitor, v_s is the steady-state rate, E_t is the total enzyme concentration, K_i' is the apparent inhibition constant, and x is a factor that when multiplied with I will yield the molar concentration of the inhibitor. It was shown before (Vicentini et al., 1990) that K_i' is related to the dissociation constant K_i by

$$K_i' = K_i(1 + S/K_m). \quad (2)$$

Two independent determinations were carried out for each RNase A variant.

Competition assay

The inhibition constant K_i for the RNase A–RI complex was determined in the absence of S-protein and found to be 74.3 pM. In another series of experiments, *S*-protein at 3 different concentrations was added to RI and UpA. The reaction was started by addition of RNase A (10 pM), and the time course of formation of adenosine was followed. Steady-state rate was reached after 3 h, and was determined from the adenosine concentrations at 180 and 240 min. The rates were corrected for the residual activity of the *S*-protein (0.04% of that of RNase A), and the data were analyzed as described by Stone et al. (1987).

Acknowledgments

We thank R. Matthies for sequencing the RNase variants, R. Steiner (Biocenter, University of Basel) for help with the CD spectra, W. Zürcher (Ciba, Basel) for performing the mass spectra, and Drs. J. Fominaya and H. Angliker (Friedrich Miescher-Institut, Basel) for critically reading the manuscript.

References

Betz A, Hofsteenge J, Stone SR. 1991. Ionic interactions in the formation of the thrombin-hirudin complex. *Biochem J 275*:801-803.

Blackburn P, Gavilanes JG. 1982. Identification of lysine residues in the binding domain of ribonuclease A for the RNase inhibitor from human placenta. *J Biol Chem 257*:316-321.

Blackburn P, Jailkhani BL. 1979. Ribonuclease inhibitor from human placenta: Interaction with derivatives of ribonuclease A. *J Biol Chem 254*: 12488-12493.

Bond MD, Vallee BL. 1990. Replacement of residues 8-22 of angiogenin with 7-21 of RNase A selectively affects protein synthesis inhibition and angiogenesis. *Biochemistry 29*:3341-3349.

Chaiken IM. 1981. Semisynthetic peptides and proteins. *Crit Rev Biochem 11*:255-301.

Charbonneau H. 1989. Strategies for obtaining partial amino acid sequence data from small quantities (<5 nmol) of pure or partially purified protein. In: Matsudaira PT, ed. *A practical guide to protein and peptide purification for microsequencing*. New York: Academic Press. pp 15-30.

de Llorens R, Arus C, Parés X, Cuchillo CM. 1989. Chemical and computer graphic studies on the topography of the ribonuclease active-site cleft. A model of the enzyme-pentanucleotide substrate complex. *Protein Eng 2*:417-429.

Doscher MS, Hirs CHW. 1967. The heterogeneity of bovine pancreatic ribonuclease S. *Biochemistry 6*:304-312.

Ellman JA, Mendel D, Schultz PG. 1992. Site-specific incorporation of novel backbone structures into proteins. *Science 255*:197-200.

Fersht A, Winter G. 1992. Protein engineering. *Trends Biochem Sci 17*:292-294.

Fominaya JM, Hofsteenge J. 1992. Inactivation of ribonuclease inhibitor by thiol-disulfide exchange. *J Biol Chem 267*:24655-24660.

Haydock K, Lim C, Brünger AT, Karplus M. 1990. Simulation analysis of structures on the reaction pathway of RNase A. *J Am Chem Soc 112*:3826-3831.

Heinrikson RL. 1971. The selective *S*-methylation of sulfhydryl groups in proteins and peptides with methyl-*p*-nitrobenzenesulfonate. *J Biol Chem 246*:4090-4096.

Hofsteenge J, Kieffer B, Matthies R, Hemmings BA, Stone SR. 1988. Amino acid sequence of the ribonuclease inhibitor from porcine liver reveals the presence of leucine-rich repeats. *Biochemistry 27*:8537-8544.

Hofsteenge J, Servis C, Stone SR. 1991b. Studies on the interaction of ribonuclease inhibitor with pancreatic ribonuclease involving differential labeling of cysteinyl residues. *J Biol Chem 266*:24198-24204.

Hofsteenge J, Vicentini AM, Stone SR. 1991a. Purification and characterization of truncated ribonuclease inhibitor. *Biochem J 275*:541-543.

Homandberg GA, Komoriya A, Juillerat M, Chaiken IM. 1979. Enzymatic conversion of selected noncovalent complexes of native or synthetic fragments to covalent forms. In: Gross E, Meienhofer J, eds. *Peptides: Structure and biological function*. Rockford, Illinois: Pierce Chemical Company. pp 597-600.

Homandberg GA, Laskowski M Jr. 1979. Enzymatic resynthesis of the hydrolyzed peptide bond(s) in ribonuclease S. *Biochemistry 18*:586-592.

Homandberg GA, Mattis JA, Laskowski M Jr. 1978. Synthesis of peptide bonds by proteinases. Addition of organic cosolvents shifts peptide bond equilibria toward synthesis. *Biochemistry 17*:5220-5227.

Irie M, Ohgi K, Yoshinaga M, Yanagida T, Okada Y, Teno N. 1986. Roles of lysine$_1$ and lysine$_7$ residues of bovine pancreatic ribonuclease in the enzymatic activity. *J Biochem (Tokyo) 100*:1057-1063.

Irie M, Watanabe H, Ohgi K, Tobe M, Matsumaru G, Arata Y, Hirose T, Inayama S. 1984. Some evidence suggesting the existence of P_2 and B_3 sites in the active site of bovine pancreatic ribonuclease A. *J Biochem (Tokyo) 95*:751-759.

Knecht R, Chang JY. 1986. Liquid chromatographic determination of amino acids after gas-phase hydrolysis and derivatization with (dimethylamino)-azobenzenesulfonyl chloride. *Anal Chem 58*:2375-2379.

Kobe B, Deisenhofer J. 1993. Crystal structure of porcine ribonuclease inhibitor, a protein with leucine-rich repeats: A novel class of α/β structure. *Protein Sci 2(Suppl 1)*:144 [Abstr].

Lee FS, Shapiro R, Vallee BL. 1989. Tight-binding inhibition of angiogenin and ribonuclease A by placental ribonuclease inhibitor. *Biochemistry 28*:225-230.

Lee FS, Vallee BL. 1990. Kinetic characterization of two active mutants of placental ribonuclease inhibitor that lack internal repeats. *Biochemistry 29*:6633-6638.

Lee FS, Vallee BL. 1993. Structure and action of mammalian ribonuclease (angiogenin) inhibitor. *Progr Nucleic Acids Res 44*:1-30.

McPherson A, Brayer G, Morrison R. 1986. Crystal structure of RNase A complexed with $d(pA)_4$. *J Mol Biol 189*:305-327.

Parés X, Noques V, de Llorens R, Cuchillo CM. 1991. Structure and function of ribonuclease A binding subsites. *Essays Biochem 26*:89-103.

Richards FM, Vithayathil PJ. 1959. The preparation of subtilisin-modified ribonuclease and the separation of the peptide and protein components. *J Biol Chem 234*:1459-1465.

Richards FM, Wykoff HW. 1971. Ribonuclease A. *The Enzymes 4*:647-806.

Rydel TJ, Tulinsky A, Bode W, Huber R. 1991. Refined structure of the hirudin-thrombin complex. *J Mol Biol 221*:583-601.

Santoro J, Gonzales C, Bruix M, Neira JL, Nieto JL, Herranz J, Rico M. 1993. High-resolution three-dimensional structure of ribonuclease A in solution by nuclear magnetic resonance spectroscopy. *J Mol Biol 229*: 722-734.

Schwartz WE, Smith PK, Royer GP. 1980. *N*-(β-iodoethyl)trifluoroacetamide: A new reagent for the aminoethylation of thiol groups in proteins. *Anal Biochem 106*:43-48.

Shapiro R, Vallee BL. 1991. Interaction of human placental ribonuclease with placental ribonuclease inhibitor. *Biochemistry 30*:2246-2255.

Shapiro R, Vallee BL. 1993. Identification of functional arginines in human angiogenin by site-directed mutagenesis. *Biochemistry 31*:12477-12485.

Stone SR, Braun PJ, Hofsteenge J. 1987. Identification of regions of α-thrombin involved in its interaction with hirudin. *Biochemistry 26*: 4617-4623.

Stone SR, Hofsteenge J. 1986. Kinetics of the inhibition of thrombin by hirudin. *Biochemistry 25*:4622-4628.

Vicentini AM, Kieffer B, Matthies R, Meyhack B, Hemmings BA, Stone SR, Hofsteenge J. 1990. Protein chemical and kinetic characterization of recombinant porcine ribonuclease inhibitor expressed in *Saccharomyces cerevisiae*. *Biochemistry 29*:8827-8834.

Wells JA, Powers DB, Bott RR, Graycar TB, Estell DA. 1987. Designing substrate specificity by protein engineering of electrostatic interactions. *Proc Natl Acad Sci USA 84*:1219-1223.

Wlodawer A, Bott R, Sjölin L. 1982. The refined crystal structure of ribonuclease A at 2.0 Å resolution. *J Biol Chem 257*:1325-1332.

Wlodawer A, Sathyanarayna B, Alexandratos JN, Gustchina A, Karpeisky MA, Padykovam NS. 1993. Structural investigations of the complexes of ribonuclease A with dinucleoside inhibitors. In: D'Allessio G, ed. *Ribonucleases: Chemistry, biology, biotechnology. Abstracts of the 3rd International Meeting*. Abstr L5.